

HIGH-RESOLUTION POLARIZATION OBSERVATIONS INSIDE THE SPECTRAL LINES OF MAGNETIC Ap STARS. II. OBSERVATIONS OF α^2 CANUM VENATICORUM

ERMANNO F. BORRA

Département de Physique, Université Laval; and Observatoire Astronomique du Québec

AND

ARTHUR H. VAUGHAN

Hale Observatories, Carnegie Institution of Washington, California Institute of Technology

Received 1977 June 7; accepted 1977 September 21

ABSTRACT

We present observations, obtained with a photon-counting polarimeter and a Fabry-Perot interferometer, of the circular polarization and intensity profiles across the line Fe II $\lambda 4520.2$ in the magnetic Ap star α^2 Canum Venaticorum. We discuss briefly the H_e curve obtained from our data.

Subject headings: polarization — stars: individual — stars: magnetic — stars: peculiar A — Zeeman effect

I. INTRODUCTION

Most of the measurements of stellar magnetic fields have been made using the photographic technique developed by Babcock (1960). Using this method, Babcock, Preston, and others have gathered throughout the years a wealth of observations that has greatly increased our knowledge of stellar magnetism. However, this technique suffers from rather large errors (Preston 1969) and is limited to the study of sharp-lined stars. Moreover, recently Borra (1974*a, b*) has argued on the basis of numerical models that this technique probably suffers from systematic errors that can distort the shapes of the longitudinal magnetic field (H_e) curves.

In an earlier paper (Borra and Vaughan 1977, hereafter Paper I) we have described in detail the coudé polarimeter and Fabry-Perot interferometer of the 2.5 m Mount Wilson telescope and the use of this instrument to obtain scans of the circular and linear polarization (Zeeman signatures) across the Fe II $\lambda 4520.2$ line in the magnetic Ap star β CrB. The computer modeling of these profiles can yield considerable information on the magnetic geometry of the star. In this second paper of a series we present circular polarization and intensity profiles across the Fe II $\lambda 4520.2$ line in the magnetic star α^2 Canum Venaticorum.

The star α^2 Canum Venaticorum is one of the brightest Ap stars and therefore one of the most studied. The star was discovered to be magnetic by Babcock and Burd (1952). They found a highly non-harmonic H_e curve varying between -1400 and $+1600$ gauss. The star is a light variable and also a spectacular spectrum variable. Pyper (1969) has studied in detail the magnetic and spectrum variations of the star and has derived maps of the magnetic field and of the distribution of equivalent widths of the elements over its surface.

Borra and Landstreet (1977) have published an H_e curve of α^2 CVn derived from photoelectric measurements of polarization in the wings of H β . Their curve is nearly harmonic and thus differs substantially from Pyper's and from Babcock and Burd's curves. They attribute the difference between the photoelectric and photographic H_e curves primarily to a systematic error arising in the photographic H_e curve as proposed by Borra (1974*b*), without ruling out the possibility that nonuniform surface distribution of equivalent widths may play some role. The photoelectric H_e curves were shown to be compatible with a decentered dipole model in which the decentering parameter lies between zero (a centered dipole) and $0.4 R$ (where R is the stellar radius). Because no H_s (average scalar field) measurements are available for this star, they were unable to put more stringent limits on the value of the decentering parameter, but they concluded that a value of $0.2 R$ seemed to give the best fit. In Figures 4 to 6 of the present paper we take this curve as representative of the photoelectric H_e curve for hydrogen.

II. OBSERVATIONS

The coudé polarimeter with a Fabry-Perot interferometer and the techniques of observation described in Paper I were employed to obtain the observations of α^2 CVn described in the present paper. The circular polarization and intensity scans obtained are given in Figures 1 to 3. The spectral line Fe II $\lambda 4520.2$ is scanned in steps of 0.086 \AA (equal to the half-power bandwidth of the interferometer). Each scan is identified by the magnetic phase at the midpoint of observation, computed from the ephemeris $2,419,869.72 + 5.46939E$ (Pyper 1969).

The Julian dates for each scan are listed in Table 1. The error bars displayed with each scan show 2 standard deviations ($\pm \sigma$) associated with every point

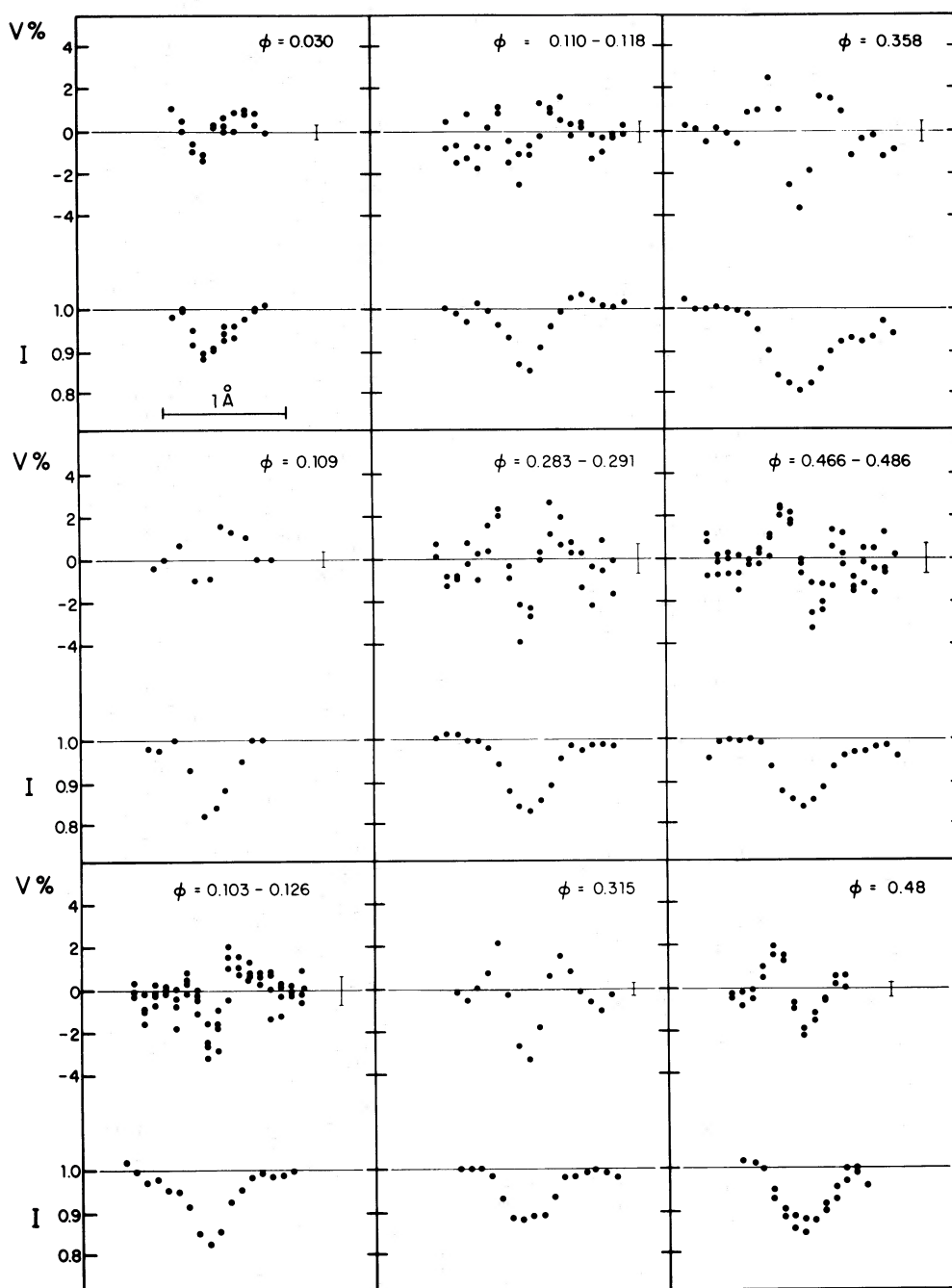


FIG. 1.—Circular polarization and line profiles obtained in Fe II $\lambda 4520.2$. Wavelength increases to the right. The wavelength scale is indicated in the first scan of the figure and is the same for all scans; the wavelength spacing between data point is 0.086 \AA . The error bars accompanying each polarization scan are equal to two standard deviations ($\pm \sigma$).

of the scan, computed on the assumption that photon shot noise is the only source of random error. Values of σ vary from scan to scan between 0.3% and 0.7% but are the same throughout a given scan. Inspection of the scans shows that the polarization observations repeat within the errors claimed. However, because we do not scan a very large range of spectrum, the location of the continuum in our line profiles is some-

what uncertain, and the statistical accuracy of our values of I/I_c , while difficult to estimate *a priori*, appears to lie in the range of 1 to 5% . Further details of the line are discussed in § III.

In Paper I we were able to draw qualitative inferences regarding the geometry of β CrB from visual inspection of the scans. In the case of α^2 CVn we are unable to do so, because rotational Doppler broadening,

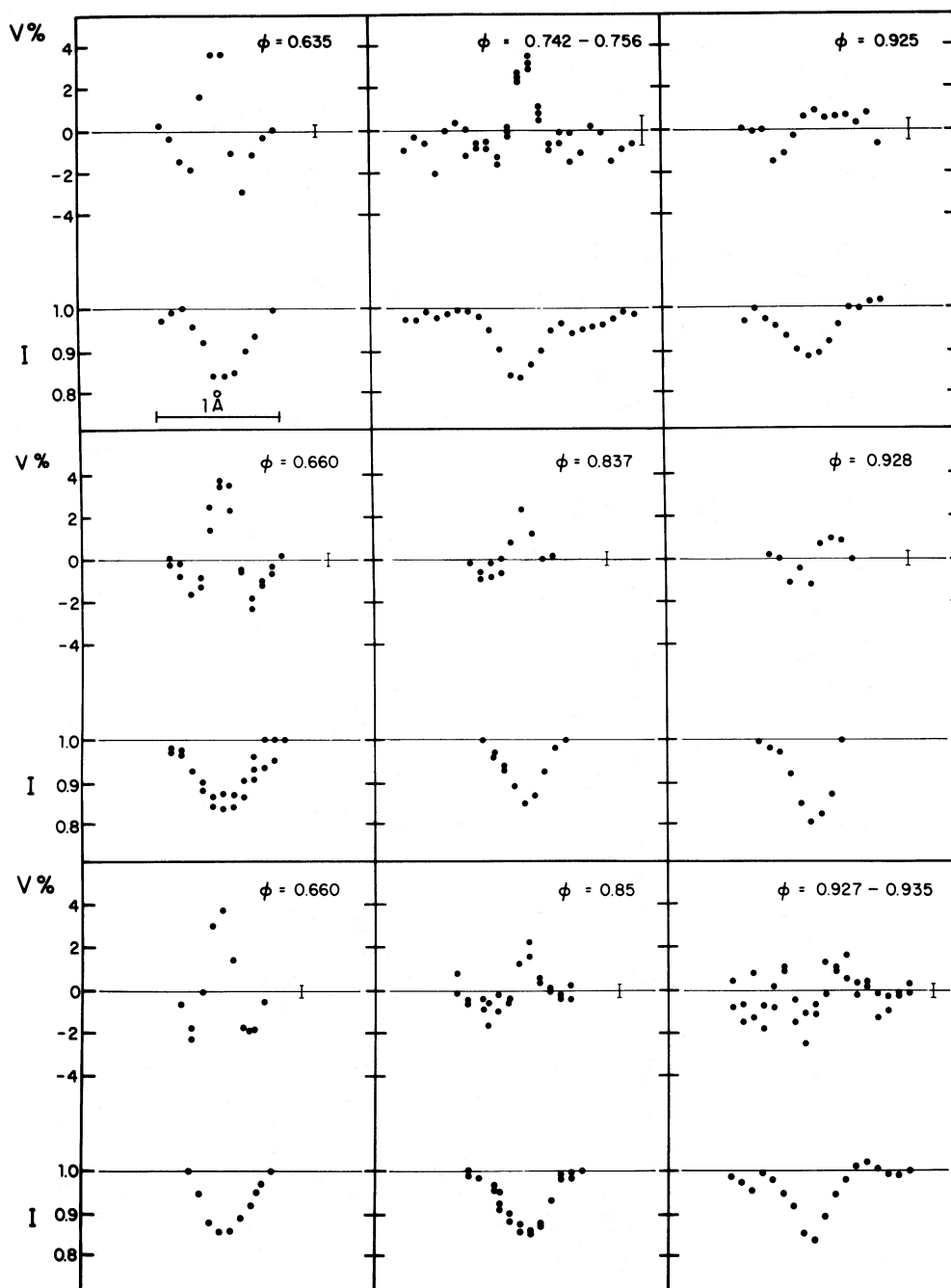


FIG. 2.—Same as Fig. 1

which tends to smooth the polarization features, is much greater in this star, and because the spectral variations introduce a still further complication. A detailed interpretation of our observations, based on numerical modeling and the oblique rotator model, is in progress and will appear elsewhere.

III. THE LONGITUDINAL MAGNETIC FIELD VARIATIONS OF α^2 CVn

From our observations we can calculate longitudinal fields H_e using both the methods described in Paper I. We will refer to these respectively as the

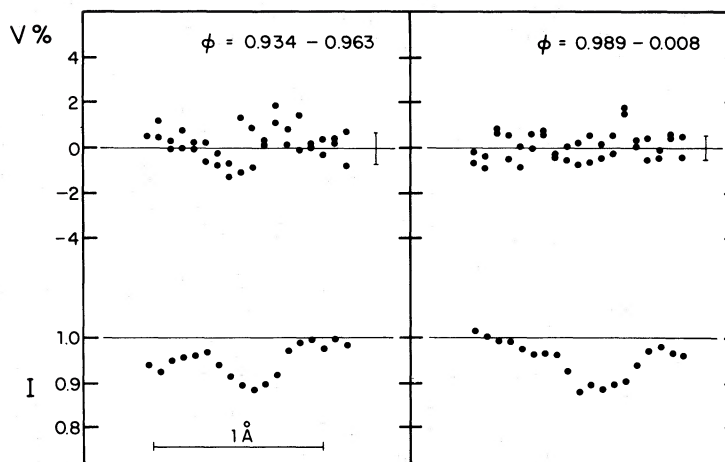


FIG. 3.—Same as Fig. 1

integral and the differential method, according to the kind of formula used. The differential method makes a least-squares fit to our data using the equation

$$V = 4.67 \cdot 10^{-13} z H_e \lambda^2 \frac{dI(\lambda)}{d\lambda} \frac{1}{I(\lambda)}, \quad (1)$$

TABLE 1
LONGITUDINAL FIELDS OBTAINED WITH THE DIFFERENTIAL AND INTEGRAL METHODS

J.D. 2,440,000+ (1)	Phase (2)	H_e Diff. (3)	H_e Int. (4)
2195.813	0.008	-676	-438
1785.730	0.030	-984	-1281
1785.730	0.030	-913	-1041
1780.658	0.103	-1057	-449
1758.813	0.109	-1090	-713
1873.677	0.110	-715	-948
1780.729	0.116	-744	-763
1873.720	0.118	-917	-1229
1780.784	0.126	-1368	-1513
1781.646	0.283	-254	+17
1781.688	0.291	-646	-413
2142.803	0.316	+884	-75
2197.729	0.358	+322	+234
1782.646	0.466	+1915	+1340
1782.726	0.481	+1160	+1706
1782.757	0.486	+1069	+661
2143.713	0.482	+1342	+698
2143.713	0.482	+995	+159
1739.817	0.635	+1397	+510
1783.708	0.660	+85	+598
2144.715	0.665	+166	+744
2144.715	0.665	-347	-275
1871.667	0.742	-1209	-1019
1871.694	0.747	-1279	-878
1871.739	0.756	-1321	-909
1784.672	0.837	-1104	-900
2145.710	0.847	-1141	-671
2145.710	0.847	-887	-1002
1872.665	0.925	-1354	-1720
1757.825	0.928	-526	-566
1779.737	0.934	-1272	-1275
1779.896	0.963	-1118	-759
2195.708	0.989	+67	-162

where z is the z -factor of the line ($z = 1.5$ for Fe II $\lambda 4520.2$), H_e is the longitudinal field strength in gauss, $I(\lambda)$ is the intensity profile normalized to 1.0 at the continuum, λ is the wavelength expressed in angstroms, and V is the fractional polarization. The integral method makes use of the integral equation

$$\Delta\lambda = \frac{\int \lambda V_c(\lambda) d\lambda}{\int r_I(\lambda) d\lambda}, \quad (2)$$

where

$$r_I(\lambda) = 1 - I(\lambda) \quad (3a)$$

and

$$V_c(\lambda) = V(\lambda)I(\lambda)10^{-2}. \quad (3b)$$

Note that in Figures 1 through 3 we display $V(\lambda)$, the percentage polarization in units of the intensity at the wavelength observed. The longitudinal field H_e is then given by

$$\Delta\lambda = 4.67 \times 10^{-13} z H_e \lambda^2. \quad (4)$$

A more detailed discussion of the methods and a justification of equation (2) is given in Paper I. In Table 1 (col. [4]) and Figure 4 we present the H_e values obtained with the integral method. Table 1 (col. [3]) and Figure 5 show the H_e values obtained with the differential method. In the same two figures we have plotted a line (*solid*) showing a fit to the photoelectric H_e values obtained by Borra and Landstreet (1977) from hydrogen (H β). The dashed lines in Figures 4 and 5 show Pyper's (1969) photographic H_e curve for her group 2 lines (a weighted mean of Ti II, Cr II, and Fe II lines).

Our scans usually extend beyond the far wings of the line. To obtain the H_e values for the line, we have to decide how much of the scan is in the line and therefore how much of it to include in the computations. Some error is introduced if the cutoff is misapplied. Our estimates of the cutoff are based on the visual appearance of the data: when it appears that there is no more line and no more polarization, we cut off. This cutoff error is important mostly with the

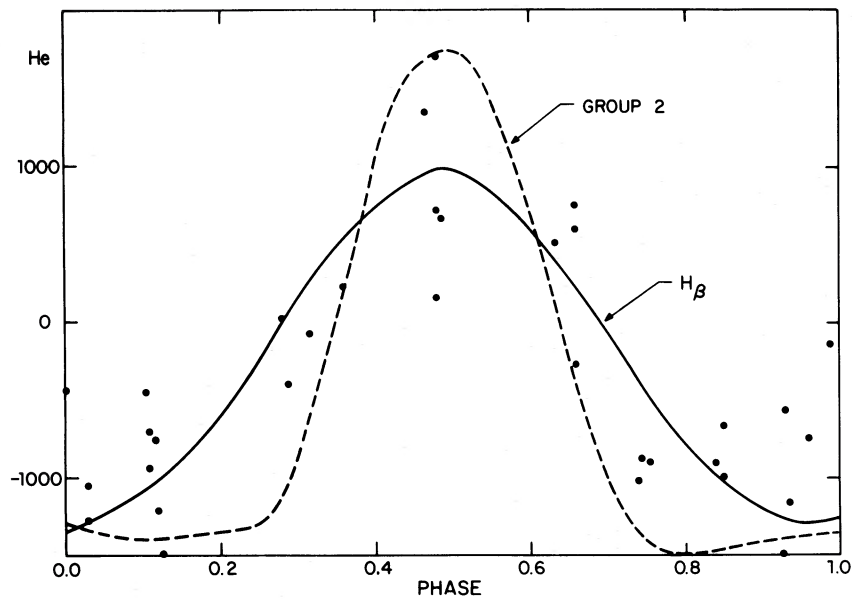


FIG. 4.—Longitudinal magnetic fields (H_e) in gauss obtained with the integral method. The continuous line shows the photoelectric H_e curve obtained in $H\beta$ by Borra and Landstreet (1977). The dashed line shows the group 2 H_e curve from Pyper (1969).

integral method. An incorrect location of the continuum also introduces errors in the values of H_e computed with the integral method because it affects the value of $\int r_1(\lambda)d\lambda$. To obtain an estimate of the standard errors in Figure 4, we have drawn a smooth line through the data, and from the deviations from it we find the standard error to be about 400 gauss. In a similar fashion we find the error in Figure 5 also to be about 400 gauss.

To compare our H_e values with Pyper's for group 2 and with the $H\beta$ curve we have made a χ^2 test (32

degrees of freedom) for the goodness of fit. The $H\beta$ curve seems to be a better representation for both the differential ($\chi^2 = 1.8$ versus 2.5) and the integral method ($\chi^2 = 1.6$ versus 3.4) than Pyper's curve. However, one should use caution in interpreting the χ^2 test. The reduced χ^2 values are high, which probably indicates that the standard deviations used (400 gauss) are too low. Moreover, we have assumed that all H_e values have the same standard deviation. This is probably not the case, as the numerical errors (see Paper I) are likely to be larger near crossover, and all

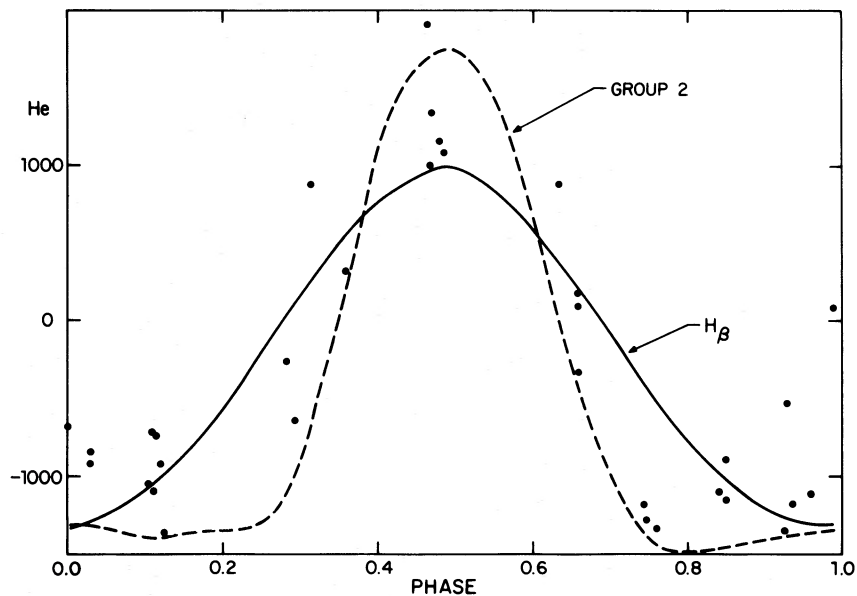


FIG. 5.— H_e values obtained with the differential method. The symbols are the same as in Fig. 4.

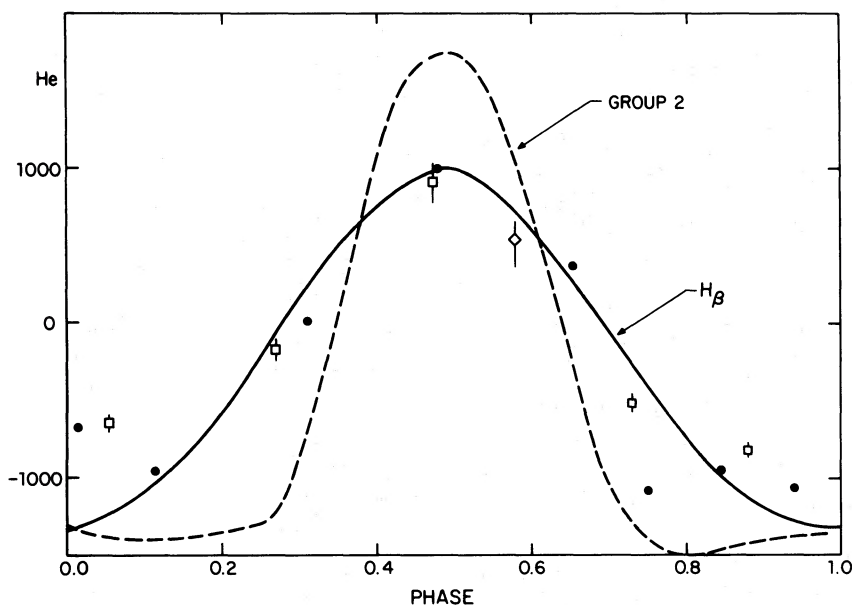


FIG. 6.—The dots show mean H_e values from our Fe II $\lambda 4520.2$ data. The squares and diamond show H_e values in Fe II $\lambda 4923.9$ and Fe II $\lambda 4233$ by Landstreet (1976). See text for more details. The full and dashed lines are the same as in Figs. 4 and 5.

the scans do not have the same accuracy in V . Finally, we have not proved that the “numerical noise” is of a totally statistical nature. We have tried to reduce the noise in those figures by averaging H_e values taken very near to each other in phase, the logical assumption being that in doing this the observational errors will be smaller. These average values are tabulated in Table 2: the first column gives the number of scans in the average, the second gives the mean phase, the third the average value of H_e from the integral method, and the fourth the average from the differential method. Further, because there does not seem to be a systematic difference between the two sets of values, we take an additional mean between the two: this is tabulated in the last column of Table 2 and is plotted in Figure 6. In the same figure, we have plotted H_e values obtained by Landstreet (1976) in α^2 CVn from Fe II $\lambda 4233$ (diamond) and Fe II $\lambda 4923.92$ (squares) with yet a different photoelectric method (see Borra and Landstreet 1973). Landstreet observed, alternatively, one point in the blue wing and one point in the red wing of the line with a bandpass slightly smaller than the width of the wing. The magnetic field is then obtained from the average polarization $\langle V \rangle = (V_{\text{red}} - V_{\text{blue}})/2$ and equation (1) with the appropriate values. The error bars indicate the standard deviations from photon statistics alone. Our data agree well with Landstreet’s. The Fe II photoelectric curve defined by our data and Landstreet’s better fits the $H\beta$ curve than Pyper’s group 2 curve which should be representative of Fe II. It is only near negative extremum that our and Landstreet’s data deviate from the $H\beta$ curve. This is shown more clearly if we compare Figure 7a, where we have plotted the difference ΔH_e between the photoelectric Fe II H_e (ours and Landstreet’s) and Pyper’s curve for group 2, with

Figure 7b, where we have done the same between the photoelectric Fe II H_e and the $H\beta$ curves. The deviations are considerably smaller in Figure 7b, and it would thus appear that our and Landstreet’s data support the arguments presented by Borra (1974b) and Borra and Landstreet (1977).

However, there are some difficulties in determining the exact shape of the Fe II H_e curve. Our errors are large, and an examination of Table 1 shows that occasionally some value of H_e deviates considerably from its expected value; this is caused by “numerical noise”: an uncertainty in the numerical computations due to insufficient sampling (Paper I). The H_e values obtained near crossover, especially with the differential method, are the least reliable. The H_e values are sensitive to the subjective cutoff used and to the location of the continuum. Finally, there is the possibility of blends with other spectral lines, especially near the far wings. For all these reasons we cannot draw definitive conclusions as to the exact shape of our H_e

TABLE 2
MEAN VALUES OF THE LONGITUDINAL FIELD

Number Obs. (1)	Phase (2)	H_e Diff. (3)	H_e Int. (4)	$\langle H_e \rangle$ (5)
4.....	0.015	-627	-731	-679
6.....	0.114	-982	-936	-959
4.....	0.312	+77	-59	+9
5.....	0.479	+1087	+912	+1000
4.....	0.654	+326	+394	+360
3.....	0.748	-1269	-935	-1102
3.....	0.846	-1040	-858	-949
4.....	0.938	-1050	-1080	-1065

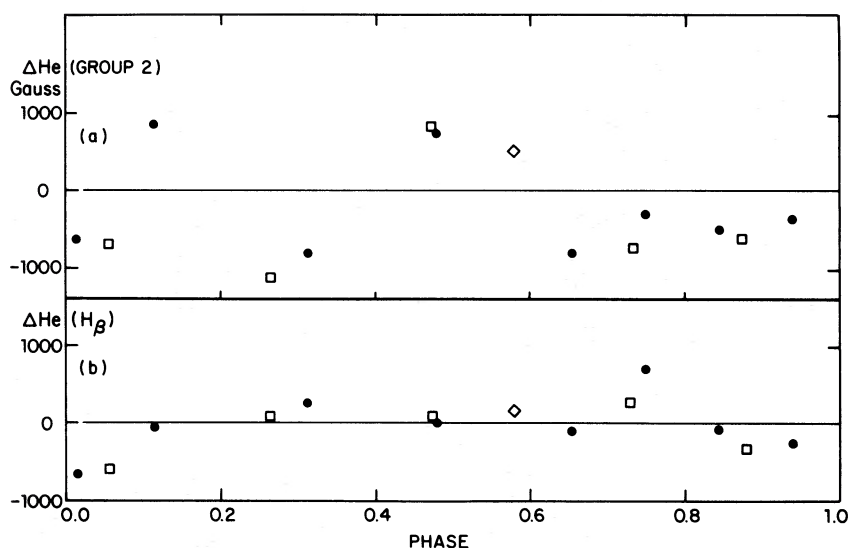


FIG. 7a (upper).—Deviations ΔH_e between the Fe II $\lambda 4520.2$ (dots), Fe II $\lambda 4233$ (diamond), Fe II $\lambda 4923.9$ (squares) longitudinal fields in Fig. 6 and Pyper's group 2 curve.

FIG. 7(b) (lower).—Same as Fig. 7(a) but the deviations are with respect to the $H\beta$ curve.

curve. To do this, we shall have to await detailed numerical modeling of the profiles (in progress).

IV. CONCLUSIONS

We have obtained circular polarization and intensity profiles across the $\lambda 4520.2$ Fe II line in α^2 CVn, throughout its magnetic cycle. The shapes of the polarization profiles vary greatly throughout the cycle. Because the star rotates relatively rapidly, and because of the additional complication introduced by the spectrum variations, we cannot draw simple inferences regarding the magnetic geometry of the star from a visual inspection of the scans. We shall have to await detailed computer modeling. The mean longi-

tudinal H_e fields derived from our data follow the harmonic photoelectric H_e curve obtained in hydrogen by Borra and Landstreet (1977) better than Pyper's (1969) highly nonharmonic photographic H_e curve. The H_e values obtained by Landstreet (1976) in other Fe II lines and with a different method also agree with our data.

We would like to thank Dr. J. D. Landstreet for communicating to us his observations in advance of publication. One of us (E. F. B.) wishes to thank the Carnegie Institution of Washington for the support of a Carnegie Postdoctoral Fellowship during most of this investigation. This research was supported in part by the National Research Council of Canada.

REFERENCES

- Babcock, H. W. 1960, in *Stellar Atmospheres*, ed. J. L. Greenstein (Chicago: University of Chicago Press).
 Babcock, H. W., and Burd, S. 1952, *Ap. J.*, **116**, 8.
 Borra, E. F. 1974a, *Ap. J.*, **187**, 271.
 ———. 1974b, *Ap. J.*, **188**, 287.
 Borra, E. F., and Landstreet, J. D. 1973, *Ap. J. (Letters)*, **185**, L139.
 Borra, E. F., and Landstreet, J. D. 1977, *Ap. J.*, **212**, 141.
 Borra, E. F., and Vaughan, A. H. 1977, *Ap. J.*, **216**, 462 (Paper I).
 Landstreet, J. D. 1976, private communication.
 Preston, G. W. 1969, *Ap. J.*, **158**, 1081.
 Pyper, D. M. 1969, *Ap. J. Suppl.*, **18**, 347.

ERMANNO F. BORRA: Département de Physique, Université Laval, Québec G1K 7P4, Canada

ARTHUR H. VAUGHAN: Hale Observatories, 813 Santa Barbara St., Pasadena, CA 91101